

Experimental and Theoretical Characterization of the Oxygen-Coordinated Donor–Acceptor Adducts of COCl₂, COClF, and COF₂ with AsF₅ and SbF₅

Berthold Hoge,^{†,§} Jerry A. Boatz,[‡] Joachim Hegge,[†] and Karl O. Christe^{*,†,‡}

Loker Hydrocarbon Research Institute, University of Southern California, Los Angeles, California 90089-1661, and Air Force Research Laboratory, Edwards Air Force Base, California 93524

Received February 8, 1999

When reacted with an excess of the corresponding carbonyl halides, AsF₅ and SbF₅ form the following 1:1 adducts: COCl₂·AsF₅, COCl₂·SbF₅, COClF·AsF₅, COClF·SbF₅, COF₂·AsF₅, and COF₂·SbF₅. All adducts are unstable at ambient temperature, and their dissociation enthalpies were determined from the dissociation pressure curves. Vibrational and multinuclear NMR spectra and theoretical calculations show that all compounds are oxygen-coordinated donor–acceptor adducts, and that the strengths of the oxygen bridges increase from COF₂ to COCl₂ and from AsF₅ to SbF₅. Full normal coordinate analyses of the adducts demonstrate that the bridging modes occur below 100 cm⁻¹, justifying the frequently used approximation of analyzing similar weak adducts in terms of their separate donor and acceptor molecules.

Introduction

In the course of an investigation of halocarbonyl cations,¹ it became necessary to study the competing Lewis base–Lewis acid interactions of the dihalocarbonyl compounds, COCl₂, COClF, and COF₂, with AsF₅ and SbF₅. Although the individual dihalocarbonyl and Lewis acid molecules are well characterized, little is known about their interactions.²

For COCl₂, no reports on the AsF₅/COCl₂ system were found, and the only report on the SbF₅/COCl₂ system consists of a brief comment³ that with a 5-fold excess of SbF₅ in SO₂ClF solution at –78 °C a new signal was observed in the ¹³C NMR spectrum, which was correctly attributed to the COCl⁺ cation.¹ Other Lewis acids, which were studied in connection with COCl₂, include BF₃, BCl₃, AlCl₃, AlBr₃, GaCl₃, SnCl₄, SbCl₅, MoCl₆, WCl₆, and PtCl₄,² but only for AlCl₃^{4,5} and possibly SbCl₅^{4,6} was evidence presented for the existence of oxygen-coordinated 1:1 donor–acceptor adducts.

For COClF, the only reports on an interaction with Lewis acids are two NMR studies^{3,7} with SbF₅ in SO₂ClF solution. The results from these studies indicate the presence of an oxygen-coordinated donor–acceptor adduct at low temperatures and halogen exchange at higher temperatures.

For COF₂, the presence of thermally unstable, oxygen-coordinated donor–acceptor complexes with SbF₅ and AsF₅ were first demonstrated by low-temperature ¹⁹F NMR measurements,⁷ and subsequently confirmed by low-temperature Raman spectroscopy.⁸ However, no physical properties were reported for these adducts, and no reports could be found on other COF₂·Lewis acid adducts.

Experimental Section

Materials and Methods. Carbonyl chloride (Matheson), COF₂ (PCR Research Chemicals), and AsF₅ (Ozark Mahoning) were used as received. Antimony pentafluoride (Ozark Mahoning) was distilled prior to use. The COClF was prepared by a literature method.¹¹

The volatile materials were handled in a stainless steel vacuum line equipped with Teflon-FEP U-traps, 316 stainless steel bellows seal valves, and a Heise pressure gauge.⁹ Nonvolatile materials were handled in the dry nitrogen atmosphere of a glovebox. Raman spectra were recorded on a Cary model 83 GT using 1.5 W of the 488 nm exciting line of an Ar ion laser and flame-sealed Pyrex tubes as sample containers. A previously described¹⁰ device was used for the recording of the low-temperature spectra. Infrared spectra were recorded on a Midac M FTIR spectrometer. NMR spectra were measured on a Varian Unity 300 MHz NMR spectrometer equipped with a 5 mm variable-temperature broad band probe. Sealed capillaries, which were filled with acetone-*d*₆ as lock substance, TMS as ¹³C reference, and CFCl₃ or C₆H₅CF₃ as ¹⁹F reference, were placed inside the NMR tubes with the listed ¹⁹F shifts referenced to CFCl₃. For the NMR measurements, the corresponding adducts were prepared in 0.5" o.d. Teflon ampule using an excess of carbonyl halide, followed by removal of the excess at low temperature, transfer of the solid at –196 °C into an NMR tube in the dry box and addition of the solvent on the vacuum line.

For the dissociation pressure measurements, the 1:1 adducts of AsF₅ and SbF₅ with the carbonyl halides were performed in a Teflon-FEP ampule, which was directly connected to a Heise pressure gauge. The

[†] University of Southern California.

[‡] Air Force Research Laboratory.

[§] Current address: Institute of Inorganic Chemistry, University of Cologne, Germany.

(1) Christe, K. O.; Hoge, B.; Boatz, J. A.; Prakash, G. K. S.; Olah, G. A.; Sheehy, J. A. *Inorg. Chem.*, in press.

(2) For a recent review, see: Ryan, T. A.; Ryan, C.; Seddon, E. A.; Seddon, K. R. *Phosgene and Related Carbonyl Halides*; Topics in Inorganic and General Chemistry, Monograph 24; Clark, R. J. H., Ed.; Elsevier: Amsterdam, 1996.

(3) Prakash, G. K. S.; Bausch, J. W.; Olah, G. A. *J. Am. Chem. Soc.* **1991**, *113*, 3203.

(4) Christe, K. O. *Inorg. Chem.* **1967**, *6*, 1706.

(5) Huston, J. L. *J. Inorg. Nucl. Chem.* **1956**, *2*, 128.

(6) Dehnicke, K. *Z. Anorg. Allg. Chem.* **1961**, *312*, 237.

(7) Bacon, J.; Dean, P. A. W.; Gillespie, R. J. *Can. J. Chem.* **1971**, *49*, 1276.

(8) Chen, G. S. H.; Passmore *J. Chem. Soc., Dalton Trans.* **1979**, 1257.

(9) Christe, K. O.; Wilson, R. D.; Schack, C. *J. Inorg. Synth.* **1986**, *24*, 3.

(10) Miller, F. A.; Harney, B. M. *Appl. Spectrosc.* **1969**, *23*, 8.

(11) Hoge, B.; Christe, K. O. *J. Fluor. Chem.* **1999**, *94*, 107.

equilibrium dissociation pressures were established for each temperature, approaching the equilibria from both sides, i.e., higher pressures and lower pressures. The thermochemical properties were derived in the same manner as previously described.¹² The method used for the tensiometric titration (vapor pressure–composition isotherm) of the AsF₅–COF₂ system has previously been described.⁴

Preparation of COF₂·AsF₅. Arsenic pentafluoride (3.75 mmol) and COF₂ (40.0 mmol) were combined in a 3/4" o.d. Teflon-FEP ampule at –196 °C. The mixture was stirred at –78 °C for 1 h with a magnetic stirring bar, resulting in a suspension of a white solid in liquid COF₂. The excess of COF₂ was pumped off at –126 °C, leaving behind the white, solid COF₂·AsF₅ adduct in quantitative yield. The adduct melts in the range of –45 to –42 °C. Dissociation pressure (temperature [°C], pressure [mm]): (–100, 2), (–95, 4), (–90, 7), (–85, 13), (–81, 20), (–75, 38), (–71, 58), (–70, 66), (–66, 98), (–65, 108), (–64, 119), (–63, 131), (–62, 140), (–60, 168), (–57, 211), (–55, 253). NMR (SO₂ClF, –60 °C) for COF₂·AsF₅: δ(¹³C) 137.8 ppm; ¹J(¹³C–¹⁹F) 330 Hz; δ(¹⁹F) 16 ppm. For COF₂: δ(¹³C) 130.0 ppm; ¹J(¹³C–¹⁹F) 313 Hz; δ(¹⁹F) 23 ppm.

Preparation of COF₂·SbF₅. A mixture of SbF₅ (16.8 mmol) and COF₂ (40.0 mmol) was reacted, and the resulting white, solid 1:1 adduct isolated as described for COF₂·AsF₅. The yield of COF₂·SbF₅ was quantitative.

Preparation of COClF·AsF₅. A mixture of AsF₅ (1.7 mmol) and COClF (30.2 mmol) was stirred at –78 °C for 1 h. The excess of COClF was pumped off at –110 °C, leaving behind COClF·AsF₅ (1.7 mmol) as a white, solid powder melting in the range –42 to –39 °C. Dissociation pressure (temperature [°C], pressure [mm]): (–87, 3), (–84, 4), (–82, 5), (–80, 6), (–79, 7), (–78, 8), (–77, 9), (–76, 10), (–75, 11), (–74, 14), (–73, 16), (–72, 18), (–71, 20), (–70, 22), (–69, 25), (–68, 28), (–67, 32), (–66, 35), (–65, 39), (–64, 44), (–63, 50), (–62, 56), (–61, 62), (–60, 68), (–59, 76), (–58, 85), (–57, 94), (–56, 104), (–55, 117), (–54, 128), (–53, 140), (–52, 157), (–51, 170), (–50, 192), (–49, 224), (–48, 247), (–47, 275), (–46, 298), (–45, 320), (–44, 342), (–43, 363), (–42, 380).

Preparation of COClF·SbF₅. A mixture of SbF₅ (2.3 mmol) and COClF (15.6 mmol) was reacted as described for COClF·AsF₅, resulting in the quantitative formation of the white, solid COClF·SbF₅ adduct. NMR (SO₂ClF, –60 °C) for COClF·SbF₅: δ(¹³C) 163.8 ppm; ¹J(¹³C–¹⁹F) 383 Hz; δ(¹⁹F) 73.9 ppm. For COClF: δ(¹³C) 142.0 ppm; ¹J(¹³C–¹⁹F) 368 Hz; δ(¹⁹F) 59.7 ppm. Dissociation pressure (temperature [°C], pressure [mm]): (–43, 3), (–40, 9), (–38, 11), (–36, 14), (–34, 19), (–29, 35), (–25, 54), (–23, 70), (–20, 96), (–16, 139), (–15, 152), (–13, 173), (–12, 187), (–11, 194), (–10, 200).

Preparation of COCl₂·AsF₅. A mixture of AsF₅ (12.0 mmol) and COCl₂ (30.0 mmol) was stirred at –78 °C for 1 h. The excess of COCl₂ was pumped off at –85 °C, leaving behind 3.2 g of a white solid (weight calcd for 12.0 mmol of COCl₂·AsF₅ = 3.226 g), melting at –20 ± 2 °C. NMR (SO₂ClF, –60 °C) for COCl₂·AsF₅: δ(¹³C) 155.9 ppm. For COCl₂: δ(¹³C) 143.7 ppm. Dissociation pressure (temperature [°C], pressure [mm]): (–63, 5), (–60, 9), (–58, 12), (–51, 22), (–44, 49), (–43, 59), (–42, 66), (–40, 85), (–38, 104), (–37, 115), (–35, 143), (–32, 186), (–29, 230), (–28, 260), (–27, 292), (–26, 330), (–25, 375), (–24, 421), (–22, 481).

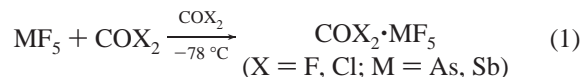
Preparation of COCl₂·SbF₅. Antimony pentafluoride (4.3 mmol) was dissolved at –78 °C in 5 mL of liquid COCl₂. After 5 min the solution became turbid and a precipitate formed. After 1.5 h, the excess of COCl₂ was pumped off at –78 °C, leaving behind 4.3 mmol of COCl₂·SbF₅ in the form of a white powder. Dissociation pressure and NMR data could not be measured due to rapid F–Cl exchange resulting in COClF formation.

Computational Methods. The optimized geometries, vibrational spectra and NMR chemical shifts of the O-coordinated carbonyl halide·MF₅ (M = As, Sb) adducts were calculated using density functional methods. The B3LYP hybrid functional¹³ and the Stevens, Basch, Krauss, Jasien, and Cundari effective core potentials and the corre-

sponding valence double-ζ basis sets¹⁴ were used. The basis set was augmented with a diffuse s+p shell¹⁵ and a single Cartesian d polarization function on each atom.¹⁶ These calculations, hereafter denoted as B3LYP/SBK+(d), were performed using Gaussian 94 and 98.¹⁷ The calculated Hessian matrixes (second derivatives of the energy with respect to Cartesian coordinates) were converted to symmetry-adapted internal coordinates for further analysis with the program systems GAMESS¹⁸ and Bmtrix.¹⁹

Results and Discussion

Synthesis and Properties of the COX₂·MF₅ (X = Cl, F; M = As, Sb) Adducts. Both SbF₅ and AsF₅ form with an excess of either COCl₂, COClF or COF₂ exclusively O-coordinated 1:1 donor–acceptor complexes (eq 1).



The 1:1 compositions were established by the observed material balances and for the COF₂/AsF₅ system by a tensiometric titration (vapor pressure–composition isotherm)⁴ at –78 °C which gave evidence only for a 1:1 adduct. The resulting adducts are white solids which are thermally unstable and decompose reversibly to the starting materials, except for the COCl₂/SbF₅ system for which rapid irreversible fluorine–chlorine exchange is observed (eq 2).¹¹



The oxygen-bridged nature of these adducts was established by vibrational and multinuclear NMR spectroscopy and the results

- (14) (a) Melius, C. F.; Goddard, W. A. *Phys. Rev. A* **1974**, *10*, 1528. (b) Kahn, L. R.; Baybutt, P.; Truhlar, D. G. *J. Chem. Phys.* **1976**, *65*, 3826. (c) Krauss, M.; Stevens, W. J. *Annu. Rev. Phys. Chem.* **1985**, *35*, 357. (d) Stevens, W. J.; Basch, H.; Krauss, M. *J. Chem. Phys.* **1984**, *81*, 6026. (e) Stevens, W. J.; Basch, H.; Krauss, M.; Jasien, P. *Can. J. Chem.* **1992**, *70*, 612. (f) Cundari, T. R.; Stevens, W. J. *J. Chem. Phys.* **1993**, *98*, 5555.
- (15) The diffuse s+p function exponents used for Sb, As, Cl, F, O, and C were 0.0259, 0.0287, 0.0483, 0.1076, 0.0845, and 0.0438, respectively.
- (16) The d function exponents used for As, Sb, and Cl were 0.293, 0.211, and 0.75, respectively. An exponent of 0.8 was used for F, O, and C.
- (17) (a) Frisch, M. J.; Trucks, G. W.; Schlegel, H. B.; Gill, P. M. W.; Johnson, B. G.; Robb, M. A.; Cheeseman, J. R.; Keith, T.; Petersson, G. A.; Montgomery, J. A.; Raghavachari, K.; Al-Laham, M. A.; Zakrzewski, V. G.; Ortiz, J. V.; Foresman, J. B.; Cioslowski, J.; Stefanov, B. B.; Nanayakkara, A.; Challacombe, M.; Peng, C. Y.; Ayala, P. Y.; Chen, W.; Wong, M. W.; Andres, J. L.; Replogle, E. S.; Gomperts, R.; Martin, R. L.; Fox, D. J.; Binkley, J. S.; Defrees, D. J.; Baker, J.; Stewart, J. P.; Head-Gordon, M.; Gonzalez, C.; Pople, J. A.; *Gaussian 94*, Revision E.2; Gaussian, Inc. Pittsburgh, PA, 1995. (b) Frisch, M. J.; Trucks, G. W.; Schlegel, H. B.; Scuseria, G. E.; Robb, M. A.; Cheeseman, J. R.; Zakrzewski, V. G.; Montgomery, J. A. Jr.; Stratmann, R. E.; Burant, J. C.; Dapprich, S.; Millam, J. M.; Daniels, A. D.; Kudin, J. N.; Strain, M. C.; Farkas, O.; Tomasi, J.; Barone, V.; Cossio, M.; Cammi, R.; Mennucci, B.; Pomelli, C.; Adamo, C.; Clifford, S.; Ochterski, J.; Petersson, G. A.; Ayala, P. Y.; Cui, Q.; Morokuma, K.; Malick, D. K.; Rabuck, A. D.; Raghavachari, K.; Foresman, J. B.; Cioslowski, J.; Ortiz, J. V.; Stefanov, B. B.; Liu, G.; Liashenko, A.; Piskorz, P.; Komaromi, I.; Gomperts, R.; Martin, R. L.; Fox, D. J.; Keith, T.; Al-Laham, M. A.; Peng, C. Y.; Nanayakkara, A.; Gonzalez, C.; Challacombe, M.; Gill, P. M. W.; Johnson, B.; Chen, W.; Wong, M. W.; Andres, J. L.; Gonzalez, C.; Head-Gordon, M.; Replogle, E. S.; Pople, J. A. *Gaussian 98*, Revision A.4; Gaussian, Inc.: Pittsburgh, PA, 1998.
- (18) Schmidt, M. W.; Baldridge, K. K.; Boatz, J. A.; Elbert, S. T.; Gordon, M. S.; Jensen, J. H.; Koseki, S.; Matsunaga, N.; Nguyen, K. A.; Su, S. J.; Windus, T. L.; Dupuis, M.; Montgomery, J. A. *J. Comput. Chem.* **1993**, *14*, 1347.
- (19) Komornicki, A. *Bmtrix*, version 2.0; Polyatomics Research Institute: Palo Alto, CA, 1996.

- (12) (a) Christie, K. O.; Guertin, J. P. *Inorg. Chem.* **1965**, *4*, 905. (b) Christie, K. O.; Sawodny, W. *Inorg. Chem.* **1967**, *6*, 1783; **1969**, *8*, 212.
- (13) Becke, A. D. *Chem. Phys.* **1993**, *98*, 5648.

Table 1. Thermochemical Data for the Dissociation of the X₂CO·MF₅ Donor–Acceptor Adducts and Their Heats of Formation

	H_d° ^a kcal/mol	T (1 atm) ^b °C	P_{298}° atm	F_{298}° ^d kcal/mol	S_{298}° cal/deg mol	$H_f^\circ(X_2CO \cdot AsF_5)$ kcal/mol
Cl ₂ CO·AsF ₅	22.75	-16.8	22.78	-2.882	85.98	-370.81
ClFCO·AsF ₅	19.15	-34.5	56.15	-3.951	77.49	-416.61
F ₂ CO·AsF ₅	16.17	-41.5	50.19	-3.818	67.05	-464.33
ClFCO·SbF ₅	13.91	0.6	8.07	-0.826	49.41	-433.15

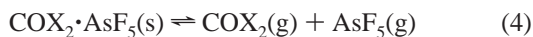
^a Enthalpies of dissociation, calculated from the slope of the log P vs T^{-1} curves. ^b Extrapolated temperatures at which the dissociation pressures of the solid adducts would reach a dissociation pressure of 760 mm. ^c Extrapolated dissociation pressures at 298 K. ^d Values for the free energy change at 298 K. ^e Values for the entropy changes at 298 K. ^f Standard heats of formation of the solid adducts using the dissociation enthalpies of this work and the following literature values for the heats of formation: $H_f^\circ(\text{COCl}_2(\text{g})) = -52,600$; $H_f^\circ(\text{COFCl}(\text{g})) = -102,000$; $H_f^\circ(\text{COF}_2(\text{g})) = -152,700$; $H_f^\circ(\text{AsF}_5(\text{g})) = -295,461$; $H_f^\circ(\text{SbF}_5(\text{l})) = -317,248$ kcal/mol.

from the theoretical calculations. Only for COCIF with at least a 3-fold excess of SbF₅ does the formation of ionic salts containing the CICO⁺ cation become energetically more favorable (eq 3).¹



The preferential formation of oxygen-coordinated 1:1 donor–acceptor adducts in these systems is in accord with the previous Raman study of the COF₂·MF₅ (M = As, Sb) systems,⁸ a ¹⁹F NMR study of the COCIF·SbF₅ system,⁷ and a tensimetric and IR spectroscopic study of the COCl₂/AlCl₃ system.⁴

Thermochemical Properties. Based on the vapor pressure data given in the Experimental Section, plots of log P versus T^{-1} for the heterogeneous equilibria (eqs 4 and 5) give straight lines,



which can be described by the following equations:

$$\text{COCl}_2 \cdot \text{AsF}_5 \text{ (210–251 K): } \log P \text{ (mm)} = -2486.13/T \text{ (K)} + 12.5768$$

$$\text{COCIF} \cdot \text{AsF}_5 \text{ (186–231 K): } \log P \text{ (mm)} = -2092.67/T \text{ (K)} + 11.649$$

$$\text{COF}_2 \cdot \text{AsF}_5 \text{ (173–218 K): } \log P \text{ (mm)} = -1767.12/T \text{ (K)} + 10.5084$$

$$\text{COCIF} \cdot \text{SbF}_5 \text{ (230–263 K): } \log P \text{ (mm)} = -3038.9/T \text{ (K)} + 13.98$$

The thermochemical properties, derived from these data by standard procedures,¹² are summarized in Table 1. Literature values were used for the required heats of formation of AsF₅,²⁰ SbF₅,²¹ and the carbonyl halides.²² Table 1 shows that the stability of the COX₂·MF₅ adducts decreases from SbF₅ to AsF₅, as expected for the decrease in Lewis acidity, and from COCl₂ to COF₂, as expected from a decreasing basicity of the oxygen with increasing electron density withdrawal by the more electronegative fluorine ligands. The decrease in the dissociation energy ΔH_d° from COCIF·AsF₅ to COCIF·SbF₅ should not be mistaken as an indication of a weaker adduct. The decrease in ΔH_d° is caused by the fact that at the investigated dissociation temperatures the SbF₅ decomposition product is a solid and not

a gas. Therefore, the value of ΔH_d° is only one-half of that expected for the formation of 2 mol of gas from 1 mol of solid. The slopes of the log P versus T^{-1} curves, which are independent of the number of moles of gas in the decomposition products, reflect the expected stability trends, i.e., COCl₂·AsF₅ > COCIF·AsF₅ > COF₂·AsF₅ and COCIF·SbF₅ > COCIF·AsF₅. The same stability trend is also displayed by the extrapolated temperature values at which the adducts would reach a dissociation pressure of one atmosphere (see Table 1). A comparison of the data of Table 1 with the previously reported⁴ dissociation pressure of 440 mm at 25 °C for COCl₂·AlCl₃ suggests that the stability of the COCl₂·AlCl₃ adduct is significantly higher than that of COCl₂·AsF₅.

NMR Spectra. The results of our ¹³C and ¹⁹F NMR study are summarized in Table 2. In agreement with a previous observation,⁷ difficulties were encountered in observing well resolved signals for some of the systems at low temperatures due to exchange phenomena. Table 2 shows that on formation of the donor–acceptor adducts both the ¹³C and ¹⁹F signals of the free carbonyl halides are shifted to lower fields, as expected from a deshielding of these nuclei by the electron-withdrawing effect of the Lewis acids. These shifts vary from about 5 to 20 ppm and appear to be larger for the stronger Lewis acid SbF₅. The magnitudes and directions of these shifts were confirmed by our theoretical calculations at the B3LYP/vdz+p level of theory using the GIAO method (see Table 2).

Since our NMR measurements were carried out at temperatures at which some of the adducts exhibit significant dissociation pressures, the possibility that the signals, observed for the carbonyl halide part of the adducts, might represent exchange-averaged spectra for an equilibrium mixture of COX₂ and COX₂·SbF₅ had to be considered. For the COF₂–SbF₅ and COCIF–SbF₅ systems it was found that the observed shifts and coupling constants of the signals, attributed to the free carbonyl halides and their SbF₅ adducts, remained unchanged whether an excess of carbonyl halide or SbF₅ was used, and only their relative intensities varied. Furthermore, in the ¹⁹F spectrum of COF₂·SbF₅ in SO₂ClF solution at -100 °C a well-resolved AX₄ pattern, characteristic for coordinated SbF₅,⁷ was observed (δ -109.3, doublet, area of 4; δ -142.4, quintet, area of 1; ¹J(F–F) = 96 Hz), indicating that the observed COF₂·SbF₅ spectrum was not influenced by exchange processes. In addition to the COF₂·SbF₅ signals, a separate resonance due to free non-exchanging COF₂ was observed at -179 ppm in the ¹⁹F spectrum.

The previously reported^{3,7} NMR data are for the most part ambiguous. Thus, the report³ on the COCIF·SbF₅ adduct in SO₂ClF at -80 °C listed only ¹³C data with a wide shift range of 150–175 ppm which do not permit a meaningful comparison with the signal of free COCIF.

The other previous report⁷ dealt only with the ¹⁹F spectra of COF₂·SbF₅, COFCl·SbF₅ and COF₂·AsF₅ in SO₂ClF solution and also contained some ambiguities. Thus, for COF₂·AsF₅ no

(20) Barin, I.; Knacke, O.; Kubaschewski, O. *Thermochemical Properties of Inorganic Substances*; Supplement, Springer-Verlag: Berlin, 1977.

(21) Bougon, R.; Bui Huy, T.; Burgess, J.; Christe, K. O.; Peacock, R. D. *J. Fluor. Chem.* **1982**, *19*, 263.

(22) JANAF *Interim Thermochemical Tables*; The Dow Chemical Co.: Midland, MI, 1965, and subsequent revisions.

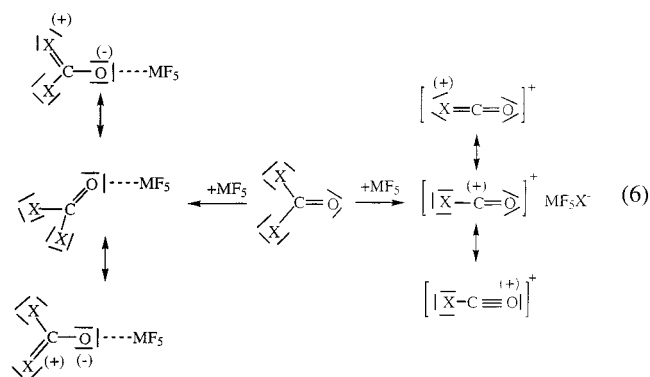
Table 2. Selected ^{13}C and ^{19}F NMR Parameters for COF_2 , COCIF , COCl_2 , and Some of their Lewis Acid Adducts

	chemical shifts (ppm)				coupling constant (Hz)
	$\delta (^{13}\text{C})$		$\delta (^{19}\text{F})$		
	obsd ^a	calcd ^b	obsd ^a	calcd ^b	
COF_2^g	130.0 (134.2) ^c	133.0	-18.3 (-23.0) ^c (-19.6) ^d	-28.7	308 (309) ^c
COCIF	142.0 (140.5) ^c	143.6	59.7 ^{a,c}	54.5	368 (366) ^c
COCl_2	143.7 (141.8) ^c	154.0	—	—	—
$\text{COF}_2 \cdot \text{AsF}_5$	137.8	137.4	-16	-20.4	330
$\text{COF}_2 \cdot \text{SbF}_5^g$	145.5	139.7	2.5 (2.1) ^d	-12.6	325
$\text{COCIF} \cdot \text{AsF}_5$	—	152.8 ^e (152.8) ^f	—	59.0 ^e (54.7) ^f	—
$\text{COCIF} \cdot \text{SbF}_5$	163.8	157.7 ^e (158.3) ^f	73.9	66.4 ^e (58.5) ^f	383
$\text{COCl}_2 \cdot \text{AsF}_5$	155.9	167.7	—	—	—
$\text{COCl}_2 \cdot \text{SbF}_5$	—	176.3	—	—	—

^a All data are from this study, unless noted otherwise, and were recorded in SO_2ClF solutions at -60°C . ^b Calculated at the B3LYP/vdz+p level using the GIAO method. "vdz+p" denotes a mixed valence double zeta plus polarization basis set, constructed as follows: SBKJC effective core potentials and valence basis sets, augmented with a diffuse s+p shell and a single Cartesian d polarization function, were used for Sb and As. The 6-311G(d) basis set was used for all other atoms. ^c Data from Gombler, W. *Spectrochim. Acta, Part A* **1981**, 37, 57. ^d Data from ref 7. ^e Isomer in which the fluorine ligand of COCIF points toward the MF_5 molecule. ^f Isomer in which the chlorine ligand points toward the MF_5 molecule. ^g Recorded in SO_2ClF at -100°C .

signal for coordinated COF_2 was observed at -100°C , leading to the incorrect conclusion that even at this low-temperature complexation must be incomplete. Furthermore, for a concentrated $\text{COCIF}/\text{SbF}_5$ solution at -80°C , only signals due to free COF_2 and $\text{COF}_2 \cdot \text{SbF}_5$ were observed, while for a dilute solution at -95°C a signal at 59.9 ppm was attributed to $\text{COCIF} \cdot \text{SbF}_5$. However, this shift is almost identical to that of 59.7 ppm found in our study for free COCIF and is quite different from that of 73.9 ppm, found by us for the $\text{COCIF} \cdot \text{SbF}_5$ adduct. The previous report by Bacon, Dean, and Gillespie on the $\text{COF}_2 \cdot \text{SbF}_5$ adduct in SO_2ClF solution at -100°C using an excess of SbF_5 ⁷ is in excellent agreement with our findings (see Table 2) using either stoichiometric amounts or an excess of COF_2 . In all cases, the shift of the COF_2 signal in the adduct was about 21 ppm downfield from that of free COF_2 . It supports our conclusion that the stronger Lewis acid SbF_5 deshields the fluorine ligands of the coordinated carbonyl halides more strongly than AsF_5 . Inspection of the $^1J(^{13}\text{C}-^{19}\text{F})$ coupling constants of Table 2 shows that the C-F coupling increases upon complexation. This is in accord with the increased C-X bond strengths of the adducts, as shown by the valence bond structure (eq 6).

Vibrational Spectra and Theoretical Calculations. Vibrational spectra are well suited to distinguish between ionic salts and covalent donor-acceptor adducts.^{1,23} As shown by the valence bond structures (eq 6), the C-O and C-X bond orders



and, therefore, also their stretching frequencies decrease and the C-X stretching frequencies increase, compared to the free

(23) Lindquist, I. *Inorganic Adduct Molecules of Oxo-Compounds. In Anorganische und Allgemeine Chemie in Einzeldarstellungen*, Becke-Goehring, M., Ed.; Academic Press Inc.: New York, 1963; Band IV.

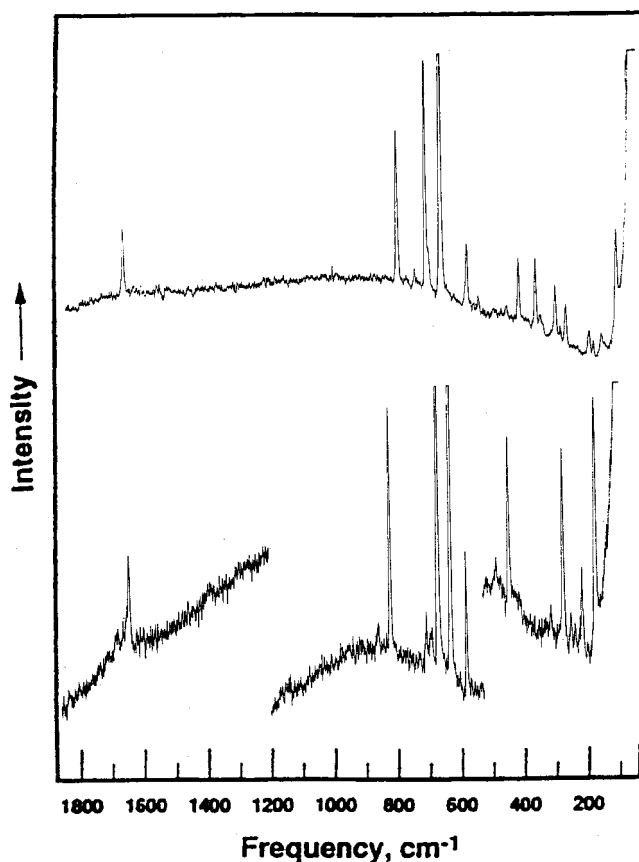


Figure 1. Raman spectra of solid $\text{COCl}_2 \cdot \text{AsF}_5$ (upper trace) and $\text{COCl}_2 \cdot \text{SbF}_5$ (lower trace) recorded at -130°C .

COX_2 molecule. Furthermore, a $\text{COX}^+\text{SbF}_5\text{X}^-$ salt should exhibit only 18 normal modes, while a covalent donor-acceptor adduct should possess 24.

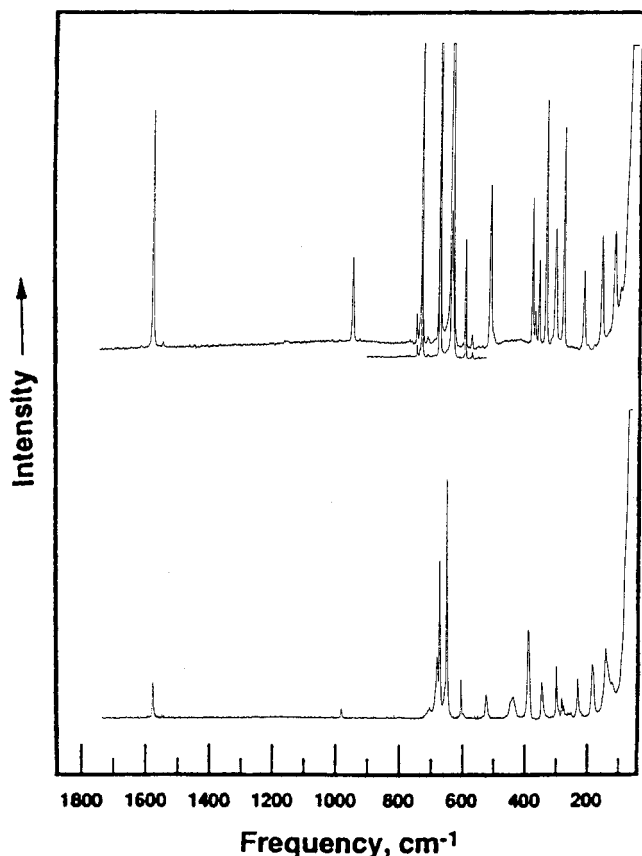
The observed low-temperature Raman spectra of the solid 1:1 complexes of Cl_2CO and ClFCO with AsF_5 and SbF_5 are shown in Figures 1 and 2, and the observed frequencies are summarized in Tables 3 and 4. The large number of observed Raman bands, their frequency shifts relative to the free carbonyl halides,²⁴ and the excellent fit with the calculated frequencies and intensities (see Tables 3 and 4) leave no doubt that these complexes are O-coordinated donor-acceptor adducts.

Traditionally, the vibrational spectra of this type of covalent donor-acceptor adducts have been analyzed in terms of their

Table 3. Calculated (B3LYP/SBK+(d) Vibrational Frequencies and Observed Raman Spectra of the $\text{COCl}_2 \cdot \text{MF}_5$ ($M = \text{As}, \text{Sb}$) Adducts and Their Analyses Based on the Point Groups of the Adducts and the Individual Donor and Acceptor Molecules

assignments, approx. mode descript			freq, cm^{-1} , intensities ^a			
$\text{MF}_5 C_{4v}$	$\text{COCl}_2 C_{2v}$	$\text{COCl}_2 \cdot \text{MF}_5 C_s$	$\text{COCl}_2 \cdot \text{AsF}_5$		$\text{COCl}_2 \cdot \text{SbF}_5^c$	
			obsd Ra	calcd (IR)[Ra]	obsd Ra	calcd (IR) [Ra]
	$\nu_1(\text{A}_1)$ 1827	$\nu(\text{A}') \nu \text{ C}=\text{O}$	1610[33]	1768(671)[43]	1587[14]	1718(740)[29]
	$\nu_4(\text{B}_1)$ 849	$\nu_2(\text{A}') \nu \text{ as CCl}_2$	978[11]	896(460)[9.7]	989[3.4]	930(430)[6.1]
$\nu_{7(\text{E})}$		$\nu_3(\text{A}') \nu \text{ as MF}_4$	770[4]	734(127)[0.35]	708[2]	667(90)[2.2]
		$\nu_{16}(\text{A}'') \nu \text{ as MF}_4$	733[1]	736(152)[0.09]	—	667(114)[0.13]
$\nu_1(\text{A}_1)$		$\nu_4(\text{A}') \nu \text{ MF}'$	757[44]	742(153)[8.3]	683[22]	665(114)[5.5]
$\nu_2(\text{A}_1)$		$\nu_5(\text{A}') \nu \text{ s MF}_4 \text{ in phase}$	698[100]	663(1.7)[30]	654[100]	617(5.7)[34]
	$\nu_2(\text{A}_1)$ 567	$\nu_6(\text{A}') \nu \text{ s CCl}_2$	660[52]	597(8.4)[16.4]	676[66]	623(0.27)[3.9]
$\nu_4(\text{B}_1)$		$\nu_{17}(\text{A}'') \nu \text{ s MF}_4 \text{ out of phase}$	615[15]	597(0.21)[2.8]	608[16]	577(0.34)[2.3]
	$\nu_6(\text{B}_2)$ 580	$\nu_{18}(\text{A}'') \delta \text{ MOCCl out of plane}$	592[2]	582(3.3)[0.02]	600sh	585(3.3)[0.08]
	$\nu_5(\text{B}_1)$ 440	$\nu_7(\text{A}') \delta \text{ MOCCl in plane}$	538[22]	471(0.25)[4.6]	528[9]	484(2.7)[4.1]
$\nu_3(\text{A}_1)$		$\nu_8(\text{A}') \delta \text{ sciss MF}_4$	402[19]	403(0.03)[1.6]	303[0.21]	307(0.12)[1.5]
$\nu_8(\text{E})$		$\nu_{19}(\text{A}'') \delta \text{ FMF}_4 \text{ out of plane}$	391[4]	380(47)[0.26]	286[8]	287(53)[0.34]
		$\nu_9(\text{A}') \delta \text{ FMF}_4 \text{ in plane}$	380[11]	379(42)[0.33]	279[4]	283(46)[0.18]
	$\nu_3(\text{A}_1)$ 285	$\nu_{10}(\text{A}') \delta \text{ sciss CCl}_2$	360[33]	308(46)[4.2]	394[37]	322(2.7)[5.1]
$\nu_6(\text{B}_2)$		$\nu_{11}(\text{A}') \delta \text{ umbrella MF}_4$	328[15]	331(83)[2.4]	260[2]	262(141)[0.17]
$\nu_9(\text{E})$		$\nu_{12}(\text{A}') \delta \text{ as MF}_4 \text{ in plane}$	304[29]	276(0.88)[1.7]	236[16]	221(0.90)[1.3]
		$\nu_{20}(\text{A}'') \delta \text{ as MF}_4 \text{ in plane}$	238[11]	278(0.63)[0.84]	—	233(0.48)[0.42]
		$\nu_{21}(\text{A}'') \delta \text{ wag COCl}_2$	181[14]	165(0.20)[0.61]	190[21]	165(0.20)[0.85]
		$\nu_{13}(\text{A}') \delta \text{ rock COCl}_2$	140[13]	125(1.2)[0.55]	146[22]	134(8.4)[0.91]
$\nu_5(\text{B}_1)$		$\nu_{22}(\text{A}'') \delta \text{ pucker MF}_4$	—	115(0)[0]	—	119(0)[0.01]
		$\nu_{14}(\text{A}') \nu \text{ M}—\text{O}$	—	74(15)[0.04]	—	104(13)[0.15]
		$\nu_{15}(\text{A}') \delta \text{ M}—\text{O}—\text{C}$	—	49(1.9)[0.36]	—	60(0.04)[0.18]
		$\nu_{23}(\text{A}'') \tau \text{ C}—\text{O}$	—	38(0.15)[1.2]	—	45(0.06)[0.88]
		$\nu_{24}(\text{A}'') \tau \text{ M}—\text{O}$	—	16(0.09)[1.2]	—	24(1.0)[1.38]

^a Calculated infrared and Raman intensities in km/mol and $\text{\AA}^4/\text{amu}$, respectively. ^b Data from ref 24. ^c In the Raman spectrum of solid $\text{COCl}_2 \cdot \text{SbF}_5$ two additional bands were observed at 442[8] and 346[15] cm^{-1} which were of variable intensity and probably do not belong to the adduct (see text).

**Figure 2.** Raman spectra of solid $\text{COClF} \cdot \text{AsF}_5$ (upper trace) and $\text{COClF} \cdot \text{SbF}_5$ (lower trace) recorded at -130°C .

separate components in their original point groups, ignoring the bridge modes and the splittings of degenerate modes caused by the symmetry lowering in the adducts. This approach has

generally been quite useful and has permitted the analysis of the gross features of the spectra, particularly when the donor–acceptor interactions are relatively weak and the splittings of the degenerate modes are small. However, a rigorous analysis of the finer details of the observed spectra requires a treatment in the correct point group of the adduct, as shown in Table 3. The resulting agreement between the observed and calculated spectra of $\text{COCl}_2 \cdot \text{AsF}_5$ is very good. The fact that the observed carbonyl stretching frequency is lower and the CCl_2 stretching frequencies are higher than those calculated indicates that in the condensed phase the interactions between the carbonyl halides and the Lewis acids are stronger than those predicted for the free gaseous adducts. Therefore, the calculated optimized geometries, shown in Figure 3, are expected to exhibit somewhat longer $\text{M}—\text{O}$ and shorter $\text{C}—\text{O}$ bonds than those expected for the condensed phase. The theoretical results furthermore predict that the modes due to the $\text{M}—\text{O}$ bridge should occur below 100 cm^{-1} and, hence, justify the traditional approach of neglecting the bridge modes in a vibrational analysis. Finally, it should be noted, that our normal coordinate analyses show that, contrary to the previous assignments⁸ and those generally given for closely related C_{4v} MF_4F species,^{25,26} the frequencies of the MF_5 deformation modes decrease in the following order: $\delta(\text{scissor}$

- (24) (a) Shimanouchi, T. *J. Phys. Chem. Ref. Data* **1977**, *6*, 993 and references therein. (b) Shimanouchi, T. *Tables of Molecular Vibrational Frequencies, Consolidated Volume 1*; NSRDS-NBS39, Nat. Stand. Ref. Data Ser.; National Bureau Standards (U.S.): Gaithersburg, MD, 1972, and references therein.
- (25) Siebert, H. *Anwendungen der Schwingungsspektroskopie in der Anorganischen Chemie. Anorganische und Allgemeine Chemie in Einzeldarstellungen*; Becke-Goehring, M., Ed.; Springer-Verlag: Berlin, 1966, Band VII.
- (26) Nakamoto, K. *Infrared and Raman Spectra of Inorganic and Coordination Compounds* 5th ed.; John Wiley & Sons: New York, 1997; Part A.

Table 4. Calculated (B3LYP/SBK + (d)) Vibrational Frequencies and Observed Raman Spectra of the COCIF·MF₅ (M = As, Sb) Adducts and Their Analyses Based on the Point Groups of the Adducts and the Individual Donor and Acceptor Molecules

assignments, approx mode descript			freq, cm ⁻¹ , intensities			
MF ₅ C _{4v}	COCIF C _s obsd ^a	COCIF·MF ₅ C _s	COCIF·AsF ₅		COCIF·SbF ₅	
			obsd Ra	calcd ^c (IR)[Ra]	obsd Ra	calcd ^c (IR)[Ra]
	$\nu_1(A')$ 1868	$\nu_1(A')$ ν C=O	1701[40]	1826(695)[38]	1669[8]	1789(751)[25]
	$\nu_2(A')$ 1095	$\nu_2(A')$ ν CF	1220[1]	1167(416)[4]	1257(vs) ^b	1208(412)[2.0]
$\nu_7(E)$		$\nu_3(A')$ ν as MF ₄	{780[5]	{735(147)[0.17]	712[2]	{667(112)[2.0]
		$\nu_{16}(A'')$ ν as MF ₄	{732[5]	{736(160)[0.06]		{670(126)[0.22]
$\nu_1(A_1)$		$\nu_4(A')$ ν MF'	742[52]	743(173)[5.8]	689[42]	668(106)[4.0]
$\nu_2(A_1)$		$\nu_5(A')$ ν s MF ₄ in phase	695[100]	663(2.2)[31]	651[100]	621(2.3)[28]
	$\nu_3(A')$ 776	$\nu_6(A')$ ν CCl	835[35]	781(47)[15]	842[21]	795(50)[13]
$\nu_4(B_1)$		$\nu_{17}(A'')$ ν s MF ₄ out of phase	616[16]	597(0.13)[3.1]	603[15]	578(0.36)[2.6]
	$\nu_6(A'')$ 667	$\nu_{18}(A'')$ δ MO CCl out of plane	580[4]	659(8.5)[0.32]	590[2]	660(2.4)[0.20]
	$\nu_4(A')$ 501	$\nu_7(A')$ δ MO CCl in plane	453[16]	520(2.1)[5.2]	470[15]	536(6.8)[3.4]
$\nu_3(A_1)$		$\nu_8(A')$ δ sciss MF ₄	401[13]	404(0.01)[1.6]	301[18]	308(0.08)[1.6]
$\nu_8(E)$		$\nu_{19}(A'')$ δ FMF ₄ out of plane	{390[4]	{380(48)[0.25]	275[3]	{287(53)[0.30]
		$\nu_9(A')$ δ FMF ₄ in plane	{382[2]	{379(43)[0.26]		{285(49)[0.29]
	$\nu_5(A')$ 415	$\nu_{10}(A')$ δ sciss ClCF	340[9]	420(0.29)[2.3]	337[3]	429(1.9)[2.4]
$\nu_6(B_2)$		$\nu_{11}(A')$ δ umbrella MF ₄	325[3]	327(125)[1.9]	265[2]	264(134)[0.27]
$\nu_9(E)$		$\nu_{12}(A')$ δ as MF ₄ in plane	{306[10]	{276(0.83)[1.0]	240[8]	{223(0.98)[0.79]
		$\nu_{20}(A'')$ δ as MF ₄ in plane	{233[5]	{278(0.69)[0.86]		{232(0.77)[0.41]
		$\nu_{21}(A'')$ δ wag COCIF	197[4]	164(0.12)[0.45]	198[20]	165(0.13)[0.73]
		$\nu_{13}(A')$ δ rock COCIF	148[17]	137(1.2)[0.13]		146(5.5)[0.60]
$\nu_5(B_1)$		$\nu_{22}(A'')$ δ pucker MF ₄		114(0)[0]		115(0)[0]
		$\nu_{14}(A')$ ν M—O		76(15)[0.21]		109(14)[0.20]
		$\nu_{15}(A')$ δ M—O—C		53(1.6)[0.31]		62(0.05)[0.27]
		$\nu_{23}(A'')$ τ C=O		36(0.13)[1.1]		41(0.06)[0.64]
		$\nu_{24}(A'')$ τ M—O		28(0.02)[0.51]		32(0.01)[0.81]

^a Data from ref 2.4. ^b Frequency and intensity from the infrared spectrum. ^c The listed calculated frequencies are for the isomers in which the fluorine atom of the COCIF unit is pointed toward MF₅.

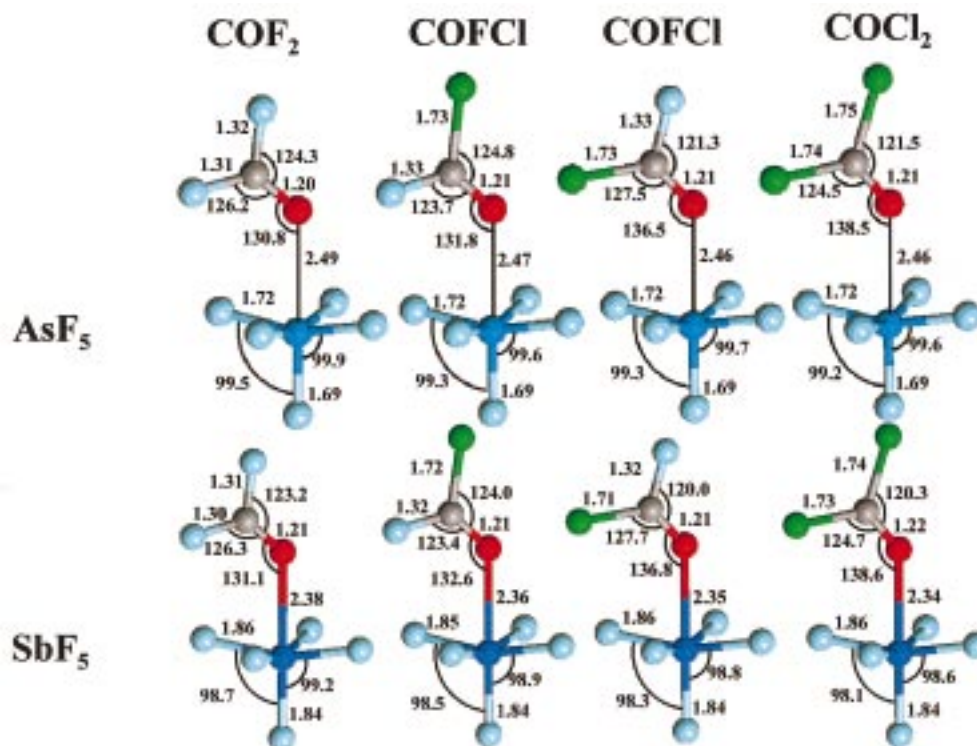


Figure 3. Geometries optimized at the B3LYP/SBK+(d) level for COCl₂·MF₅, COCIF·MF₅ and COF₂·MF₅ (M = As (Sb)). The optimized geometries of the free carbonyl halides at the same level are as follows: COCl₂, $r_{CO} = 1.195$ Å, $r_{Cl} = 1.772$ Å, $\angle OClCl = 123.8^\circ$; COCIF, $r_{CO} = 1.192$ Å, $r_{Cl} = 1.755$ Å, $r_{CF} = 1.345$ Å, $\angle OClCl = 126.6^\circ$, $\angle OCF = 123.9^\circ$; COF₂, $r_{CO} = 1.189$ Å, $r_{CF} = 1.332$ Å, $\angle OCF = 126.2^\circ$. As expected, in the adducts the C—O bonds are longer, the C—X bonds are shorter, and the O—C—X angles are smaller than in the free carbonyl halides.

MF₄ in plane) > δ (FMF₄) > δ (umbrella MF₄) > δ (asym MF₄ in plane).

The observed Raman spectra of COCl₂·MF₅ (M = As, Sb) agree very well with the calculations, except for two extra bands observed for COCl₂·SbF₅ at 442 and 346 cm⁻¹. These bands

occur in the Sb—Cl region and are tentatively attributed to some halogen exchange between COCl₂ and SbF₅ which is known¹¹ to occur rapidly at slightly elevated temperatures.

For the COCIF·MF₅ adducts, two conformers are possible because either the fluorine or the chlorine ligand of COCIF could

Table 5. Calculated (B3LYP/SBK+(d)) Vibrational Frequencies and Literature^a Raman Spectra of the COF₂·MF₅ (M = As, Sb) Adducts and Their Analyses

assignments, approx mode descript			freq, cm ⁻¹ , intensities			
MF ₅ C _{4v}	COF ₂ C _{2v} obsd ^b	COF ₂ ·MF ₅ C _s	COF ₂ ·AsF ₅		COF ₂ ·SbF ₅	
			obsd Ra	calcd (IR)[Ra]	obsd Ra	calcd (IR)[Ra]
	$\nu_1(\text{A}_1)$ 1928	$\nu_1(\text{A}') \nu$ C=O	1788[12]	1896(704)[22]	1770[9]	1866(753)[13]
	$\nu_4(\text{B}_1)$ 1249	$\nu_2(\text{A}') \nu$ as CF ₂	1402[5]	1314(407)[4.2]	1436[4]	1360(398)[3.3]
$\nu_7(\text{E})$		$\nu_3(\text{A}') \nu$ as MF ₄	776[7]	{ 736(146)[0.48]	716[19]	{ 669(108)[2.0]
		$\nu_{16}(\text{A}'') \nu$ as MF ₄	~735[7]	{ 736(117)[0.11]	701[29]	{ 669(108)[0.12]
$\nu_1(\text{A}_1)$		$\nu_4(\text{A}') \nu$ MF'	765[18]	746(142)[6.1]	673[82]	671(98)[4.1]
$\nu_2(\text{A}_1)$		$\nu_5(\text{A}') \nu$ s MF ₄ in phase	701[100]	664(2.8)[26]	658[100]	622(2.2)[23]
	$\nu_2(\text{A}_1)$ 965	$\nu_6(\text{A}') \nu$ s CF ₂	1037[20]	993(3.7)[9.8]	1050[28]	1013(26)[10]
$\nu_4(\text{B}_1)$		$\nu_{17}(\text{A}'') \nu$ s MF ₄ out of phase	615[16]	597(0.28)[3.1]	600[23]	578(0.64)[2.6]
	$\nu_6(\text{B}_2)$ 774	$\nu_{18}(\text{A}'') \delta$ MOCF ₂ out of plane	792[3]	756(74)[0.56]	774[6]	757(43)[0.52]
	$\nu_5(\text{B}_1)$ 626	$\nu_7(\text{A}') \delta$ MOCF ₂ in plane	673[4]	623(13)[1.5]	coincid. ^d	634(16)[3.3]
$\nu_3(\text{A}_1)$		$\nu_8(\text{A}') \delta$ umbrella MF ₄	406[13]	405(0.02)[1.7]	303[28]	309(0.09)[1.6]
$\nu_8(\text{E})$		$\nu_{19}(\text{A}'') \delta$ FMF ₄ out of plane	351[4] ^e	{ 381(48)[0.19]	285[5]	{ 288(52)[0.19]
		$\nu_9(\text{A}') \delta$ FMF ₄ in plane		{ 380(45)[0.20]		{ 285(50)[0.21]
	$\nu_3(\text{A}_1)$ 584	$\nu_{10}(\text{A}') \delta$ sciss CF ₂	606[4]	575(3.9)[1.0]	606 sh	581(3.0)[1.0]
$\nu_6(\text{B}_2)$		$\nu_{11}(\text{A}') \delta$ sciss MF ₄	328[7]	332(96)[0.68]	265[14]	268(101)[0.19]
$\nu_9(\text{E})$		$\nu_{12}(\text{A}') \delta$ as MF ₄ in plane	308[9]	{ 276(0.95)[1.1]	226[14]	{ 222(2.8)[0.98]
		$\nu_{20}(\text{A}'') \delta$ as MF ₄ in plane	238[4]	{ 277(0.84)[1.0]	242[14]	{ 232(1.3)[0.69]
		$\nu_{21}(\text{A}'') \delta$ wag COF ₂	—	165(0.05)[. 19]	194[19]	167(0.04)[0.37]
		$\nu_{13}(\text{A}') \delta$ rock COF ₂	—	142 (5.4)[0.07]	—	163(20)[0.17]
$\nu_5(\text{B}_1)$		$\nu_{22}(\text{A}'') \delta$ pucker MF ₄	—	108(0)[0]	—	112(0)[0]
		$\nu_{14}(\text{A}') \nu$ M—O	—	87(14)[0.15]	—	115(7.9)[0.09]
		$\nu_{15}(\text{A}') \delta$ M—O—C	—	55(0.82)[0.01]	—	65(0)[0.03]
		$\nu_{23}(\text{A}'') \tau$ C=O	—	42(0.01)[0.47]	—	47(0)[0.40]
		$\nu_{24}(\text{A}'') \tau$ M—O	—	24(0.20)[0.27]	—	34(0.20)[0.25]

^a The observed frequencies were taken from ref 8. ^b Data from ref 24. ^c Weak bands shown in the figures but not listed in the tables of ref 8. ^d Coincidence with either 658[100] or 673[82]. ^e Figure 3 of ref 8 shows weak bands in the 380 cm⁻¹ region, which might also belong to ν_{19} and ν_9 of the adduct.

be oriented toward the MF₅ group. The two conformers differ only very little in energy (~0.1 kcal/mol) and their calculated vibrational spectra are almost identical. Therefore, the observed Raman spectra do not allow to distinguish between the two conformers, and the ones with the fluorines pointing toward the MF₅ groups were chosen for our analyses (see Table 4). The MF₅ bands in their COCIF adducts agree well with those of the corresponding COCl₂ adducts, but the deviations between the observed and calculated bands for the COCIF part of the adducts are larger than those for the COCl₂ adducts.

For the COF₂·MF₅ adducts, good quality Raman spectra have previously been reported⁸ by Chen and Passmore, and their experimental data are compared with our calculations in Table 5. Again, the overall agreement is very satisfactory.

A comparison of the relative changes of the carbonyl halide stretching frequencies within the COCl₂·MF₅, COFCl·MF₅ and COF₂·MF₅ series shows that the strength of the adducts increases from COF₂ to COCl₂ and from AsF₅ to SbF₅, i.e., with increasing basicity of the donor and increasing acidity of the acceptor. Hence, COCl₂·SbF₅ is the strongest and COF₂·AsF₅ the weakest adduct within this series.

Conclusion

Even with strong Lewis acids, such as AsF₅ or SbF₅, the carbonyl halides, COCl₂, COFCl, and COF₂, preferentially form O-coordinated donor–acceptor adducts. The stability of the adducts increases with increasing basicity of the donor, i.e., from COF₂ to COCl₂, and with increasing acidity of the acceptor, i.e., from AsF₅ to SbF₅. This conclusion is strongly supported by thermochemical measurements, vibrational and multinuclear NMR spectroscopy and theoretical calculations.

Acknowledgment. The authors thank Drs. J. Sheehy and G. Olah for their support and two of us (B.H. and J.H.) the Deutsche Forschungsgemeinschaft for a stipend. The work at USC was supported by the National Science Foundation and that at the Air Force Research Laboratory by the Propulsion Directorate. The computational work was supported in part by a grant of Cray T916 time from the Army Research Laboratory Department of Defense Computing Center and a grant of IBM SP time from the Maui High Performance Computing Center under the sponsorship of the Air Force Research Laboratory.

IC990157W